Original article

Annals of Oncology 16: 1253–1267, 2005
doi:10.1093/annonc/mdi239
Published online 3 May 2005

Antitumoral actions of the anti-obesity drug orlistat (Xenical™) in breast cancer cells: blockade of cell cycle progression, promotion of apoptotic cell death and *PEA3*-mediated transcriptional repression of Her2/*neu* (*erb* B-2) oncogene

J. A. Menendez[1,2]*, L. Vellon[1,2] & R. Lupu[1,2]*

[1]*Department of Medicine, Breast Cancer Translational Research Program, Evanston Northwestern Healthcare Research Institute, Evanston, Illinois;*
[2]*Department of Medicine, Northwestern University Feinberg School of Medicine, The Lurie Comprehensive Cancer Center, Chicago, Illinois, USA*

Received 26 December 2004; accepted 6 March 2005

Background: Orlistat (Xenical™), a US Food and Drug Administration (FDA)-approved drug for bodyweight loss, has recently been demonstrated to exhibit antitumor properties towards prostate cancer cells by virtue of its ability to block the lipogenic activity of fatty acid synthase (FAS). FAS (oncogenic antigen-519) is up-regulated in about 50% of breast cancers, is an indicator of poor prognosis, and has recently been functionally associated with the Her2/*neu* (*erb* B-2) oncogene.

Materials and methods: We assessed the antitumoral effects of orlistat against the human breast cancer cell line SK-Br3, an *in vitro* paradigm of FAS and Her2/*neu* overexpression in breast cancer.

Results: Cell cycle analyses revealed that micromolar concentrations of orlistat induced, in a time- and dose-dependent manner, significant changes in the distribution of cell populations including a complete loss of G_2-M phase, S-phase accumulation and a concomitant increase in the emerging sub-G_1 (apoptotic) cells. Poly (ADP-ribose) polymerase (PARP) cleavage, an early event required for cells committed to apoptosis, was more predominant in orlistat-treated G_1 phase cells. When we characterized signaling molecules participating in the cellular events following orlistat-induced inhibition of FAS activity and preceded inhibition of breast cancer cell proliferation, a dramatic down-regulation of Her2/*neu*-coded $p185^{Her2/neu}$ oncoprotein was found in orlistat-treated SK-Br3 cells (>90% reduction). Interestingly, a significant accumulation of the DNA-binding protein PEA3, a member of the *Ets* transcription factor family that specifically targets a PEA3-binding motif present on the Her2/*neu* gene promoter and down-regulates its activity, was observed in orlistat-treated SK-Br3 cells. When a Luciferase reporter gene driven by the Her2/*neu* promoter was transiently transfected in SK-Br3 cells, orlistat exposure was found to dramatically repress the promoter activity of Her2/*neu* gene, whereas a Her2/*neu* promoter bearing a mutated binding DNA sequence was not subject to negative regulation by orlistat, thus demonstrating that the intact PEA3 binding site on the Her2/*neu* promoter is required for the orlistat-induced transcriptional repression of Her2/*neu* overexpression. RNA interference (RNAi)-mediated silencing of FAS gene expression similarly repressed Her2/*neu* gene expression in a PEA3-dependent manner, thus ruling out a role for non-FAS orlistat-mediated effects. When the combination of orlistat and the anti-Her2/*neu* antibody trastuzumab (Herceptin™) in either concurrent (orlistat + trastuzumab) or sequential (orlistat → trastuzumab; trastuzumab → orlistat) schedules was tested for synergism, addition or antagonism using the combination index (CI) method of Chou–Talalay, co-exposure of orlistat and trastuzumab demonstrated strong synergistic effects ($CI_{10-90} = 0.110–0.847$), whereas sequential exposure to orlistat followed by trastuzumab ($CI_{10-90} = 0.380–1.210$) and trastuzumab followed by orlistat ($CI_{10-90} = 0.605–1.278$) mainly showed additive or antagonistic interactions. Indeed, orlistat-induced FAS inhibition synergistically promoted apoptotic cell death when concurrently combined with trastuzumab as determined by an ELISA for histone-associated DNA fragments. Importantly, the degree of FAS expression in a panel of human breast cancer cell lines was predictive of sensitivity to orlistat-induced anti-proliferative effects as determined by a MTT-based characterization of

**Correspondence to:* Dr J. A. Menendez or Dr R. Lupu, Department of Medicine, Northwestern University Feinberg School of Medicine, The Lurie Comprehensive Cancer Center, Chicago, Illinois, USA. Tel: +1-2243647672; Fax: +1-847-570-8022; E-mail: jmenendez@enh.org; r.lupu@northwestern.edu

metabolically viable breast cancer cells. Moreover, hypersensitivity to orlistat-induced cytotoxicity was observed in MCF-7 breast cancer cells engineered to overexpress Her2/*neu* (MCF-7/Her2-18 cells), which exhibit a significant up-regulation of FAS expression and activity.

Conclusions: These findings reveal that the development of more potent and/or bioavailable orlistat's variants targeting the lipogenic activity of FAS may open a novel therapeutic avenue for treating Her2/*neu*-overexpressing breast carcinomas.

Key words: orlistat, fatty acid synthase, Her2/*neu*, PEA3, trastuzumab, breast cancer

Introduction

An intense public interest has been generated by the characterization of the US Food and Drug Administration (FDA)-approved anti-obesity drug, orlistat (tetrahydrolipstatin; marketed by Roche as Xenical™), an irreversible inhibitor of pancreatic and gastric lipases [1, 2], as a potent inhibitor of prostate tumor growth by virtue of its ability to block fatty acid synthase (FAS) activity [3]. FAS is a critical enzyme involved in the anabolic conversion of dietary carbohydrates to fatty acids in mammals [4–7]. Up-regulation of FAS activity and expression, a minor anabolic-energy-storage FAS-dependent pathway in normal cells, is a very early and nearly universal up-regulation of FAS in many human cancers and their pre-neoplastic lesions. Its association with poor clinical outcome strengthens the hypothesis that FAS is involved in the development, maintenance, and enhancement of the malignant phenotype [8–14]. In this regard, pharmacological inhibitors of FAS are increasingly receiving more attention along with the recent reports suggesting that FAS may represent a molecular bridge connecting obesity and cancer [15–17]. Thus, while overweight and obesity are associated with an increased risk of cancer development and death from all cancers [18, 19], high levels of FAS correlate with aggressive behaviors and poor prognosis in many human malignancies, including breast cancer [8–16]. Moreover, chemical FAS blockers, formerly characterized as antitumor cytotoxic agents (i.e. cerulenin, C75), may provide therapeutic moieties for the treatment of obesity as they robustly induce rapid and profound weight loss and loss of adipose mass by affecting both food intake and energy expenditure [20–22]. The reverse is also true because natural hypolipidemic agents such as the green tea component epigallocatechin-3-gallate can induce significant anti-proliferative and apoptotic effects in cancer cells by suppressing FAS [23–25].

As a part of our efforts to assess the role of FAS signaling on the survival and proliferation of breast cancer cells, we recently identified a novel bi-directional molecular linkage between breast cancer-associated FAS activity and Her2/*neu* (*erb* B-2), a well-characterized oncogene that is overexpressed in about 30% of breast carcinomas [26–28]. First, when FAS protein expression was characterized in a wide panel of human breast cancer cell lines, a positive correlation was found between high levels of FAS [29]. Secondly, Her2/*neu* overexpression stimulates the FAS gene promoter and ultimately mediates increased endogenous fatty acid biosynthesis, and this Her2/*neu*-induced FAS up-regulation is inhibitable by Her2/*neu* inhibitors such as trastuzumab [30–32]. Thirdly, pharmacological and RNA interference (RNAi)-induced inhibition of FAS activity and expression, respectively, negatively regulates Her2/*neu* oncogene expression at the transcriptional level [33]. Fourth, the degree of Her2/*neu* oncogene expression in a panel of breast cancer cell lines did predict sensitivity to chemical FAS inhibitors-induced cytotoxicity [34]. These findings, altogether, strongly suggest that a previously unrecognized bi-directional cross-talk between FAS and Her2/*neu* is taking place in human breast cancer cells.

The objective of the present study was four-fold. First, we sought to characterize the antitumoral effects of the β-lactone orlistat towards SK-Br3 breast cancer cells, which naturally overexpress orlistat target (i.e. FAS). Secondly, the ability of orlistat to block the thioesterase function of FAS was employed as an independent strategy to confirm that pharmacological inhibition of breast cancer-associated FAS activity, regardless of the mechanism of action of the chemical FAS blocker, is accompanied by the specific suppression of Her2/*neu* oncogene overexpression. Thirdly, we sought to elucidate the ultimate molecular mechanism through which FAS blockade leads to the suppression of Her2/*neu* oncogene overexpression in breast cancer cells. Fourthly, we evaluated the therapeutic value of combining orlistat and the monoclonal antibody against Her2/*neu* trastuzumab (Herceptin™). Finally, we explored the correlation of orlistat-induced cytotoxicity with the status of FAS and Her2/*neu* expression in a wide panel of human breast cancer cell lines.

Although orlistat possesses extremely low oral bioavailability and it is obvious that a novel formulation will be required for treating tumors such as breast carcinomas, the findings of this study may open a new avenue for the development of more potent and/or bioavailable orlistat's variants targeting FAS as suitable drug candidates for the management of Her2/*neu*-overexpressing breast carcinomas.

Materials and methods

Cell lines and culture conditions

The human breast cancer cell lines SK-Br3, BT-474, MDA-MB-453, MDA-MB-435, MDA-MB-231, T47D and MCF-7 were obtained from the American Type Culture Collection (ATCC). Her2/*neu*-overexpressing MCF-7/Her2 (clone 18) cells and their matched control (empty vector-transfected) MCF-7/neo cells were provided by Mien-Chie Hung (The University of Texas MD Anderson Cancer Center, Houston, TX, USA). Breast cancer cell lines were routinely grown in phenol-red containing improved MEM (IMEM; Biosource International, Camarillo, CA, USA)

containing 5% (v/v) heat-inactivated fetal bovine serum (FBS) and 2 mM L-glutamine. Cells were maintained at 37°C in a humidified atmosphere of 95% air/5% CO_2. Cells were screened periodically for *Mycoplasma* contamination.

Materials

Trastuzumab (Herceptin™) and orlistat (Xenical™) were kindly provided by the Evanston Northwestern Healthcare Hospital Pharmacy (Evanston, IL, USA). Trastuzumab was solubilized in bacteriostatic water for injection containing 1.1% benzyl alcohol (stock solution 21 mg/ml), stored at 4°C and used within 1 month. Orlistat was extracted from Xenical™ capsules (Roche Applied Sciences) by solubilizing each pill in 1 ml of ethanol. Insoluble product was removed by centrifugation (14 000 × *g* for 5 min). The supernatant yielded a solution of orlistat (250 mM), which was aliquoted and stored at −80°C until use.

The mouse monoclonal antibodies for $p185^{Her2/neu}$ (Ab-3 and Ab-5 clones) were from Oncogene Research Products (San Diego, CA, USA). Anti-β-actin goat polyclonal and anti-PEA3 (*sc*-113) mouse monoclonal antibodies were from Santa Cruz Biotechnology (Santa Cruz, CA, USA). The anti-PARP p85 fragment antibody was from Promega Corp. (Madison, WI, USA). The primary antibody for FAS immunoblotting was a mouse IgG_1 FAS monoclonal antibody (clone 23) from BD Biosciences Pharmingen (San Diego, CA, USA).

Cell cycle analysis

Adherent and detached cells were collected after trypsin detachment, washed in phosphate-buffered salt solution (PBS) and centrifugated at 1500 rpm. Cells were resuspended at 2×10^6 cells/ml in PBS and fixed in ice-cold 80% ethanol for, at least, 24 h. Fixed cells were centrifugated at 300 × *g* and each sample resuspended in propidium iodide (PI) stain buffer (0.1% Triton X-100, 200 μg of DNase-free RNase A, 20 μg of PI) in PBS for 30 min. After staining, samples were analysed using a FACScalibur (Becton Dickinson; San Diego, CA, USA) and ModFiT LT (Verity Software).

Flow cytometric analysis of Her2/*neu* expression

Cells were seeded on 100-mm plates and cultured in complete growth medium. Upon reaching 75% confluence, the cells were washed twice with pre-warmed PBS and cultured in serum-free medium overnight. Orlistat was added to the culture as specified, and incubation was carried out at 37°C up to 48 h in low-serum (0.1% FBS). Then, the specific cell surface expression of Her2/neu-coded $p185^{Her2/neu}$ oncoprotein was determined by measuring the binding of a mouse anti-Her2/*neu* antibody directed against the extracellular domain of $p185^{Her2/neu}$ (clones Ab-5). Briefly, following treatments for 48 h, cells were washed once with cold PBS and harvested by scrapping in cold PBS. The cells were pelleted and resuspended in cold PBS containing 1% FBS and then incubated with 5 μg/ml Ab-5 antibody for 1 h at 4°C. After this, the cells were washed twice with cold PBS, resuspended in cold PBS containing 1% FBS, and then incubated with a fluorescein isothiocyanate (FITC)-conjugated anti-mouse IgG secondary antibody (Jackson Immunoresearch Labs, West Grove, PA, USA) diluted 1:200 in cold PBS containing 1% FBS for 45 min at 4°C. Finally, the cells were washed once in cold PBS, and the flow cytometric analysis was performed with a FACScalibur flow cytometer (Becton Dickinson) equipped with Cell Quest Software (Becton Dickinson). The mean fluorescence signal associated with cells for labeled $p185^{Her2/neu}$ was quantified using the Geo Mean (GM) fluorescence parameter provided with the software. All observations were confirmed by at least three, independent experiments. The data are presented as means ± S.D.

Flow cytometric characterization of PARP cleavage

After being washed twice with PBS, cells were fixed in an ice-cold 1% solution of methanol-free formaldehyde in PBS for 15 min and postfixed in 80% ethanol for at least 2 h or stored at −20°C. Fixed cells were centrifugated at 300 × *g* for 3 min and ethanol was removed. The cells were then washed twice in PBS and suspended in 0.25% Triton X-100 in PBS for 10 min at room temperature to permeabilize plasma membrane. After centrifugation (300 × *g*, 5 min) the cell pellet was resuspended in 1% (w/v) solution of bovine serum album (BSA; Sigma-Chemicals, St. Louis, MO, USA) in PBS (PBS/BSA solution) for 10 min to suppress the non-specific component of the subsequent binding of antibody. The cells were centrifugated again (300 × *g*, 5 min) and the cell pellet ($<10^6$ cells) was suspended in 100 μl of PBS/BSA containing 1:200 diluted anti-PARP p89 antibody (rabbit polyclonal antibody; Cat. No. G7341, reported by the vendor to detect PARP-p89 fragment; Promega Corp., Madison, WI, USA). The cells were then incubated for 2 h at room temperature, washed twice with 1% PBS/BSA solution, resuspended in 100 μl of FITC-conjugated anti-rabbit IgG secondary antibody (Jackson Immunoresearch Labs, West Grove, PA, USA), and incubated for 30 min at room temperature (RT) in the dark. For subsequent analysis by flow cytometry cells were counterstained with 5 μg/ml of PI in the presence of 100 μg/ml of DNase-free RNase A in PBS.

Immunoblotting analyses of Her2/*neu*, PEA3 and FAS

Experimental cells were washed twice with PBS and then lysed in buffer [20 mM Tris (pH 7.5), 150 mM NaCl, 1 mM EDTA, 1 mM EGTA, 1% Triton X-100, 2.5 mM sodium pyrophosphate, 1 mM β-glycerolphosphate, 1 mM Na_3VO_4, 1 μg/ml leupeptin, 1 mM phenylmethylsufonylfluoride] for 30 min on ice. The lysates were cleared by centrifugation in an Eppendorff tube (15 min at 14 000 × *g*, 4°C). Protein content was determined against a standardized control using the Pierce Protein kit (Rockford, IL, USA). Equal amounts of protein were resuspended in 5× Laemmli sample buffer for 10 min at 70°C, subjected to electrophoresis on either 3%–8% NuPAGE Tris-Acetate (FAS, $p185^{Her2/neu}$) or 10% SDS-PAGE (PEA3) and transferred to nitrocellulose membranes. Non-specific binding on the nitrocellulose filter paper was minimized by blocking for 1 h at room temperature (RT) with TBS-T [25 mM Tris-HCl, 150 mM NaCl (pH 7.5) and 0.05% Tween-20] containing 5% (w/v) non-fat dry milk. The treated filters were washed in TBS-T and then incubated with primary antibodies for 2 h at RT in TBS-T containing 5% (w/v) non-fat dry milk. The membranes were washed in TBS-T, horseradish peroxidase-conjugated secondary antibodies in TBS-T were added for 45 min, and immunoreactive bands were detected by enhanced chemiluminiscence reagent (Pierce, Rockford, IL, USA). Blots were re-probed with an antibody for β-actin to control for protein loading and transfer. Densitometric values of protein bands were quantified using Scion Imaging Software (Scion Corp., Frederick, MD, USA).

In situ immunofluorescent staining

Cells were seeded at a density of 1 × 104 cells/well in a four-well chamber slide (Nalge Nunc International, Rochester, NY, USA). After 48 h incubation with orlistat, cells were washed with PBS, fixed in 4% paraformaldehyde in PBS for 10 min, permeabilized with 0.2% Triton X-100/PBS for 15 min, and stored overnight at 4°C with 10% horse serum in PBS. The cells were washed and then incubated for 2 h with anti-$p185^{Her2/neu}$ Ab-3 mouse monoclonal antibody diluted 1:200 in 0.05% Triton X-100/PBS. After extensive washes, the cells were incubated for 45 min with tetramethylrhodamine isothiocyanate (TRITC)-conjugated anti-mouse IgG secondary antibody (Jackson ImmunoResearch Labs) diluted 1:200 in 0.05% Triton X-100/PBS. The cells were washed five times with PBS

and mounted with VECTASHIELD + DAPI (Vector Laboratories, Burlingame, CA, USA). As controls, cells were stained with primary or secondary antibody alone. Control experiments did not display significant fluorescence in any case (data not shown). Indirect immunofluorescence was recorded on a Zeiss microscope. Images were noise-filtered, corrected for background, and prepared using Adobe Photoshop.

Her2/*neu* promoter activity

Using FuGENE 6 transfection reagent (Roche Biochemicals, Indianapolis, IN) as directed by the manufacturer, overnight serum-starved cells seeded into 24-well plates ($\sim 5 \times 104$ cells/well) were transfected in low-serum (0.1% FBS) media with 300 ng/well of the pGL2-Luciferase (Promega, Madison, WI) construct containing a luciferase reporter gene driven by either an intact Her2/*neu* promoter fragment (Her2/*neu* wild-type PEA3-binding site-luciferase) or by a mutated Her2/*neu* mutated PEA3-binding site-luciferase along with 30 ng/well of the internal control plasmid pRL-CMV, which was used to correct for transfection efficiency. After 18 h, the transfected cells were washed and then incubated with either ethanol (v/v) or orlistat in 0.1% FBS. Alternatively, cells were transiently transfected with double-stranded siRNA targeting FAS gene (see below). Approximately 48 h after treatments, luciferase activity from cell extracts was detected with a Luciferase Assay System (Promega, Madison, WI, USA) using a Victor$^{2™}$ 1420 Multilabel Counter (Perkin Elmer Life Sciences). The magnitude of activation in Her2/*neu* promoter-luciferase-transfected cells was determined after normalization of the luciferase activity in cells co-transfected with equivalent amounts of the empty pGL2-Luciferase vector lacking the Her2/neu promoter (∅-luciferase) and the internal control plasmid pRL-CMV. This control value was used to calculate the relative change in the transcriptional activities of Her2/*neu* promoter-luciferase-transfected cells in response to treatments after normalization to pRL-CMV. The activity of the wild-type promoter in untreated control cells was defined as 100%.

RNA interference-mediated silencing of the FAS gene

Synthetic sense and antisense oligonucleotides targeting FAS gene were purchased from Dharmacon RNA Technologies (Lafayette, CO, USA). This double-stranded siRNA was as follows: sense sequence, CCCUGAGAUCCCAGCGCUGdTdT; antisense sequence, CAGCGCUGGGAUCUCAGGGdTdT. The design of these siRNA oligos targeting FAS gene was based on a DNA sequence of the type AA(N_{19}) corresponding to the nucleotides 1210–1231 located 3′ to the first nucleotide of the start codon of the human FAS cDNA (AACCCTGAGATCCCAGCGCTG). Searches of the human genome database (BLAST) were carried out to ensure the sequences would not target other gene transcripts. The final concentration of siRNA FAS in the 24-well plates was 200 nM. As a non-specific siRNA control, cells were transfected with equimolar concentrations (200 nM) of a non-specific control pool (siRNA negative control) containing four pooled non-specific siRNA duplexes (Upstate Cell Signaling Solutions-Dharmacon RNA Technologies; Catalong No. D-001206–13).

Cell death ELISA

The induction of cell death was assessed using the Cell Death Detection ELISA^{PLUS} Kit obtained from Roche Molecular Biochemicals USA (Indianapolis, IN, USA). This kit uses a photometric enzyme immunoassay that quantitatively determines the formation of cytoplasmic histone-associated DNA fragments (mono- and oligonucleosomes) after apoptotic cell death. Briefly, cells (7.5×10^3/well) were grown in 96-well plates and treated, in duplicates, with trastuzumab, orlistat or trastuzumab *plus* orlistat as specified. The induction of apoptotic cell death was evaluated using cytosolic fractions obtained from pooled adherent and floating cells (obtained by centrifugation at $200 \times g$ for 10 min) by assessing the enrichment of nucleosomes in the cytoplasm using anti-histone biotin and anti-DNA peroxidase antibodies (RT for 2 h), and determined exactly as described in the manufacturer's protocol. After three washes, the peroxidase substrate was added to each well, and the plates were read at 405 nm at multiple time intervals. The enrichment of histone-DNA fragments in treated cells was expressed as a fold increase in absorbance compared with control (vehicle-treated) cells.

Cell viability

Cell viability was determined using a modified MTT reduction assay (Cell Tieter 96 Aqueous Non-Radioactive Cell Proliferation Assay, Promega Inc., Madison, WI, USA). Briefly, cells in exponential growth were harvested by trypsinization and seeded at a concentration of 3×10^3 cells/200 µl/well into 96-well plates, and allowed an overnight period for attachment. Then the medium was removed and fresh medium along with graded concentrations of orlistat in the absence or presence of trastuzumab was added to the cultures. Compounds were not renewed during the entire period of cell exposure. Following treatments (4–5 days), 96-well plates were centrifuged at $200 \times g$ for 10 min and MTS/PMS solutions was added to each well at 1/5 volume. After incubation for 3 h at 37°C in the dark, absorbances were measured at 490 nm using a multiwell plate reader. Control cells without agents were cultured using the same conditions with comparable media changes. Compounds were not renewed during the entire period of cell exposure. The cell viability effects from exposure of cells to each compound were analysed, generating concentration–effect curves as a plot of the fraction of unaffected (*surviving*) cells versus drug concentration. Dose–response curves were plotted as percentages of the control cell absorbances, which were obtained from control cells treated with appropriate concentrations of the compounds vehicles that were processed simultaneously. For each treatment, cell viability was evaluated as a percentage using the following equation:

$$(A_{490nm}\text{oftreatedsample}/A_{490nm}\text{ofuntreatedsamples}) \times 100$$

Orlistat sensitivity was expressed in terms of the concentration of the drug required for 50% decrease in cell viability (IC_{50}). Since the percentage of control absorbance was considered to be the surviving fraction of cells, the IC_{50} value was defined as the concentration of orlistat that produced 50% reduction in control absorbance (by interpolation). Data presented summarize the mean (± SD) of three independent experiments made in triplicate.

Synergy studies: median-effect (Chou–Talalay) analyses

Synergism, addition or antagonism for orlistat and trastuzumab was determined by the multiple drug analysis of Chou and Talalay, which is based on the median-effect principle. Details of this methodology have been published [35–37]. Briefly, this method involves plotting dose–effect curves for each agent and for multiply diluted, fixed ratio combinations of agents using the median-effect equation:

$$f_a/f_u = (D/D_m)^m \quad (1)$$

In this equation, D is dose, D_m is the dose required for 50% effect (e.g. 50% inhibition of cell viability, IC_{50}), f_a is the fraction affected by dose D (e.g. 0.9 if cell viability is decreased by 90%), f_u is the unaffected fraction (therefore, $f_u = 1 - f_a$), and m is a coefficient of sigmoidicity of the dose–effect curve; $m = 1$, >1 and <1 indicate hyperbolic, sigmoidal and negative sigmoidal dose–effect curves, respectively, for an inhibitory drug. Equation (1) may be rearranged as follows:

$$D_x = D_m[f_a/(1 - f_a)]^{1/m} \quad (2)$$

The parameters m and D_m are easily determined by the median-effect plot $x = \log(D)$ versus $y = \log[f_a/(1 - f_a)]$, which is based on

the logarithmic form of equation (1) and yields a straight line where m is the slope and (D_m) is the x intercept. IC_{50} values (by interpolation) and D_m values (by the median-effect plot) were usually similar. Equation (1) may thus be solved, providing the issoeffective dose (D_x) for any effect level (e.g. IC_{10} for f_a=0.1; IC_{30} for f_a=0.3; IC_{50} for f_a=0.5, and so on). For each level of cell growth inhibition, a parameter called the Combination Index (CI) was calculated according to the equation:

$$CI = (D)_{trastuzumab}/(D_x)_{trastuzumab} + (D)_{orlistat}/(D_x)_{orlistat} + \alpha[(D)_{trastuzumab}(D)_{orlistat}/(D_x)_{trastuzumab}(D_x)_{orlistat}] \quad (3)$$

where $(D_x)_{trastuzumab}$ was the dose of trastuzumab required to produce x% effect alone, and $(D)_{trastuzumab}$ was the dose of trastuzumab required to produce the same x% effect in combination with $(D)_{orlistat}$. Similarly, $(D_x)_{orlistat}$ was the dose of orlistat required to produce x% effect alone, and $(D)_{orlistat}$ was the dose required to produce the same effect in combination with $(D)_{trastuzumab}$. If the agents are mutually exclusive (e.g. similar mode of action), then α is 0 (i.e. CI is the sum of two terms); if the agents are mutually non-exclusive (e.g. independent mode of action), α is 1 (i.e. CI is the sum of two terms). If it is uncertain whether the agents act in a similar or an independent manner, the formula may be solved both ways. For simplicity, however, the third term of the Chou and Talalay equation is usually omitted and, thus, the mutually exclusive assumption (or classic isobologram) is indicated. Only the CI values obtained from the classic (mutually exclusive) calculation are therefore given in the Results section. Similar results were obtained when the complete equation was used for combination studies with trastuzumab and orlistat (data not shown). Different values of CI may be obtained by solving the equation (3) for different values of f_a (e.g. different degrees of cell toxicity). In this method, CI values <1 indicate synergy (the smaller the value, the greater the degree of synergy), values >1 indicate antagonism and values equal to 1 indicate additive effects. In our current studies, CI profiles were compared to a preset 'null' interval of 0.95–1.05 (addition), so that mean CI values >1.05 or <0.95 were interpreted as being suggestive of antagonism and synergism, respectively. Each experiment was carried out with triplicate cultures for each data and was repeated independently at least three times. The conformity of the experimental data to the median-effect principle of the mass-action law was automatically provided by the computer printout in terms of the linear correlation coefficient (r-value) of the median-effect plots. In our studies, the r-values for orlistat, trastuzumab and their combinations were all >0.95.

Statistical analysis

All observations were confirmed by at least three independent experiments. The data are presented as means ± SD. The Student's t-test (paired and unpaired) was used to evaluate the statistical significance of mean values. Statistical significance levels were P <0.05 and P <0.005. All P values are two-tailed.

Results

Tetrahydrolipstatin, which is also known as orlistat and is marketed as Xenical™, is a derivative of a natural product containing a β-lactone moiety (Figure 1A). The β-lactone can undergo nucleophilic attack on the carbonyl carbon of the lactone ring by the active site serine of the esterase in the pancreatic lipase, yielding a covalent adduct between enzyme and inhibitor [2]. Recently, orlistat was found to inhibit the thioesterase function of FAS in a selective manner for tumor-associated FAS [3]. FAS enzymatic complex, which contains seven separate enzymatic pockets, is situated as a head-to-tail dimer with the ketoacyl synthase (KS) and malonyl (MT)/acetyl transferase (AT) domains of one monomer working together with the dehydratase (DE), enoyl reductase (ER), ketoacyl reductase (KR), acyl carrier protein (ACP), and thioesterase (TE) domains on the adjacent monomer (Figure 1B). These enzymatic domains act sequentially to condense acetyl-CoA with malonyl-CoA to form a four-carbon intermediate [5–7]. Six additional turns of the enzyme's cycle convert this intermediate to palmitate, which is then liberated from FAS by the action of the thioesterase domain [38]. Because FAS functions as a head-to-tail dimer, targeted inhibition of one of the enzymatic domains of FAS can ablate the activity of one or both FAS subunits [5, 7]. Cerulenin, a natural mycotoxin, is an antagonist of the β-ketoacyl synthase

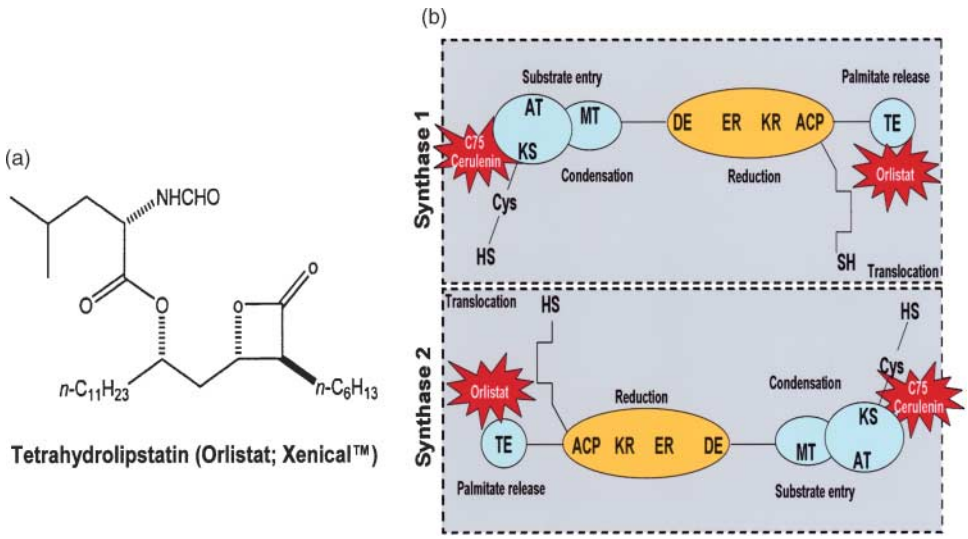

Figure 1. (**A**) Structure of the β-lactone tetrahydrolipstatin (orlistat). (**B**) Schematic representation of FAS enzymatic complex and target sites of chemical FAS blockers cerulenin, C75, and orlistat.

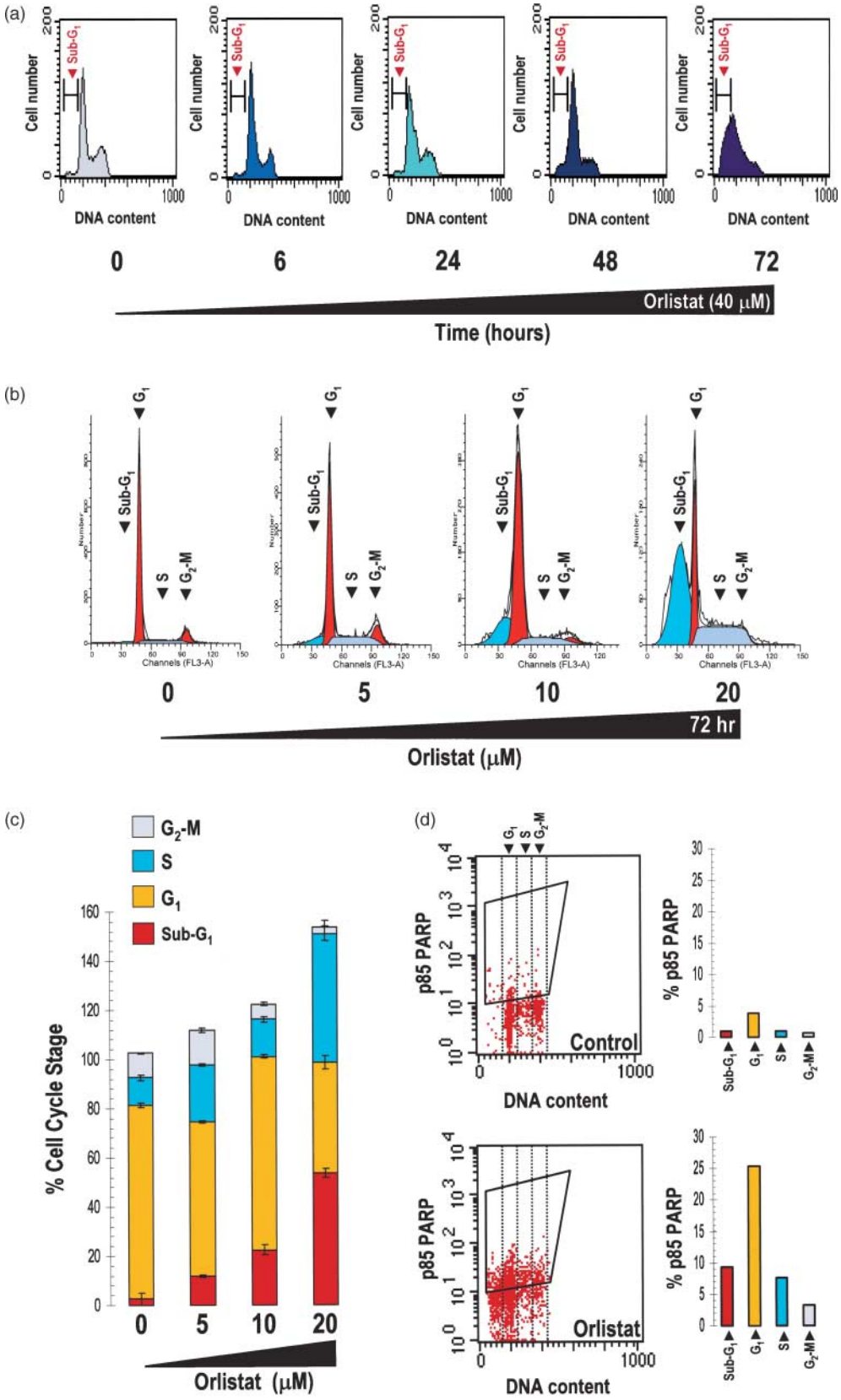

Figure 2. Effects of orlistat on cell cycle progression in SK-Br3 breast cancer cells. (**A**) After an overnight period of serum starvation and refeeding with IMEM-0.1% FBS at time 0, SK-Br3 breast cancer cells were exposed to 40 μM orlistat and analyzed at various time points. The distribution of cells in different phases of the cell cycle was monitored as a function of time using flow cytometry. The panels show representative flow cytometry profiles obtained from three independent experiments. (**B**) Distribution of SK-Br3 cells in the different cell cycle compartments was analysed by flow cytometry

domain (the condensing enzyme) of FAS and functions by covalently modifying the active site cysteine, resulting in dead-end inhibition [39]. C75, a synthetic analog of cerulenin, also targets the condensing enzyme and inhibits fatty acid synthesis [40]. These two chemical FAS inhibitors suppress tumor cell proliferation, induce tumor cell apoptosis, and slow the growth of xenograft tumors, thus supporting the notion that FAS is a relevant drug target in oncology [40–45]. Orlistat has recently been characterized as a potent and selective inhibitor of FAS in prostate carcinomas cells and, unlike cerulenin and C75, orlistat elicits its effects by inhibiting the thioesterase domain of FAS, which is responsible for releasing palmitate from the enzyme's acyl carrier protein [3, 46].

Orlistat induces blockade of cell cycle progression

To determine the effects of orlistat on breast cancer cell-cycle progression, SK-Br3 cells, after an overnight starvation period in media without serum, were exposed to a saturating concentration of orlistat (40 μM) in low-serum (0.1% FBS) conditions. The distribution of cells in different phases of the cell cycle was assessed at 6, 24, 48 and 72 h using flow cytometry. The time-dependent response of SK-Br3 breast cancer cells to orlistat was characterized by a loss of the G_2-M population, as well as an accumulation of cells in the S-phase of cell cycle. Importantly, orlistat exposure substantially promoted apoptosis as evidenced by a time-dependent accumulation of sub-G_1 populations that has <2N DNA and represents dead cells (Figure 2A).

A more detailed analysis of cell-cycle distribution was performed in SK-Br3 cells incubated for 72 h with increasing concentrations of orlistat (0–20 μM) using the ModFiT LT software (Figure 2B, C). Orlistat-induced inhibition of FAS activity produced, in a dose-dependent manner, a dramatic reduction in the proportion of G_2-M cells (from 10% in untreated control cells to 2.5% in the presence of 20 μM orlistat), while it significantly increased the proportion of S-phase cells by five-fold (from 11% in untreated control cells to 53% in the presence of 20 μM orlistat). Moreover, a dramatic dose-dependent increase in sub-G_1 (apoptotic) cells was observed following exposure to increasing concentrations of orlistat (up to 54% compared with 3% in untreated control cells).

Most of the fatty acids produced by tumor cells are incorporated into membrane phospholipids, and phospholipid synthesis is inhibited when fatty acid synthesis is inhibited [47, 48]. Phospholipid biosynthesis is greatest during the G_1 and S phases, with doubling of the membrane mass occurring during S phase in preparation for cell division [49]. Indeed, most of the phospholipid accumulation in preparation for mitosis takes place during the S phase [49]. Our current results demonstrating the ability of orlistat to arrest the cell cycle at the G_1-S transition in breast cancer cells strongly indicates that orlistat and other orlistat-related β-lactones, through its ability to disrupt the endogenous fatty acid metabolism, should be considered to be a promising class of novel chemotherapeutics that could be exploited for anti-breast cancer therapy.

Orlistat promotes apoptotic cell death of SK-Br3 breast cancer cells

Poly(ADP-ribose) polymerase (PARP), a nuclear enzyme involved in DNA repair and activated in response to DNA-damage, is an early target of caspases during apoptosis [50–52]. The specific cleavage of this protein by caspase-3 onto 89- and 24 kDa fragments is considered to be a hallmark of the apoptotic mode of cell death [50–53]. Here, PARP cleavage was detected immunocytochemically using an antibody that recognizes its 89-kDA fragment (PARP p89). The frequency and extent of PARP cleavage in its cell-cycle position was measured by multiparameter flow cytometry [54]. Figure 2D presents bivariate distributions (scatter-plots) representing immunufluorescence of PARP p89 versus DNA content of SK-Br3 cells treated with 20 μM orlistat for 72 h. Although cells from all phases of the cycle showed evidence of increased PARP cleavage in orlistat-treated cells, it was quite evident that PARP cleavage was more selective to cells progressing to the G_1 phase. Thus, this analysis revealed that the percentage of G_1 phase cells exhibiting PARP cleavage was about six-fold higher compared with G_1-associated PARP cleavage in the untreated population. These findings, together with the above results demonstrating a decline in the G_1 population of orlistat-treated cells, reveal that orlistat-induced FAS blockade does not promote arrest in G_0-G_1 as breast cancer cells are prompted to apoptosis as revealed by the degradation of PARP.

Orlistat down-regulates $p185^{Her2/neu}$ expression

Since we previously demonstrated that chemical FAS inhibitors cerulenin and C75 strongly repressed Her2/*neu* oncogene overexpression in cancer cells [33], we here evaluated whether orlistat-induced FAS blockade similarly promoted down-regulation of Her2/neu expression in SK-Br3 breast cancer cells. Flow cytometric analyses using a monoclonal antibody directed against the extracellular domain of Her2/*neu* (Ab-5; Figure 3A) established the ability of orlistat to dramatically decrease the expression levels of cell surface-associated Her2/*neu* in SK-Br3 (up to 90% reduction; Figure 3B).

Although $p185^{Her2/neu}$ is a transmembrane oncoprotein, its cytoplasmic domain can also function as a nuclear transcriptional activator [55, 56]. Therefore, we analyzed the impact of

after 72 h in the presence of graded concentrations of orlistat (0, 5, 10 and 20 μM). The distribution of cells in different phases of the cell cycle was monitored as a function of time using the ModFiT LT software. Representative cell cycle profiles (n=3) are shown for each treatment. (**C**) Cell cycle percentages for SK-Br3 cells treated with 20 μM orlistat for 72 h. (**D**) Left panels: bivariate PARP p89 immunofluoresence versus DNA content distributions (scatterplots) of SK-Br3 cells which were untreated (top panel) as well as treated with 20 μM orlistat (bottom panel) for 72 h. Right panels: percentages of PARP p89 in each cell cycle phase. Standard deviation in each experimental condition was less than 2% after three independent experiments.

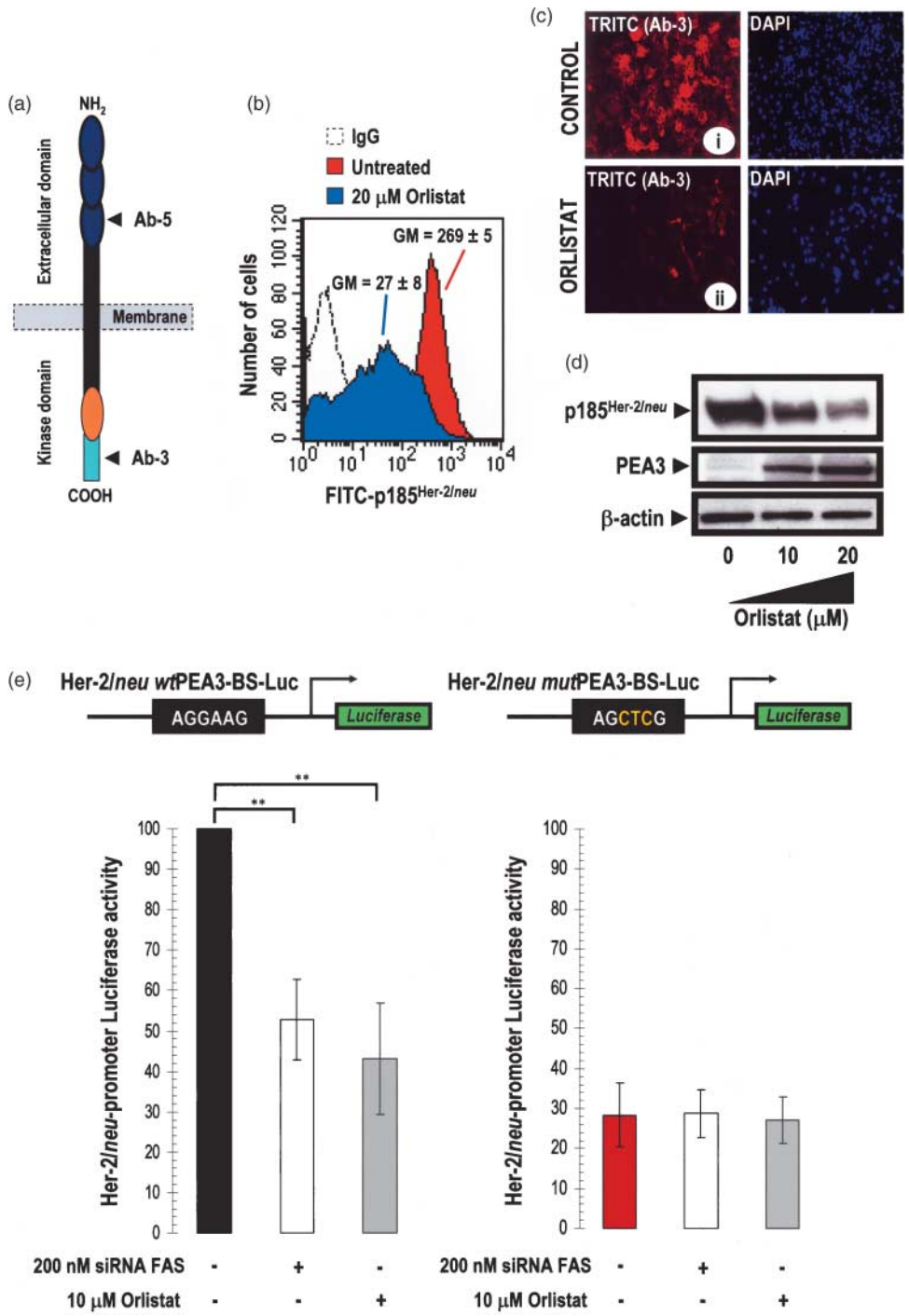

Figure 3. Orlistat suppresses Her2/*neu* overexpression in SK-Br3 breast cancer cells. (**A**) c-*erb* B-2 map showing the epitopes for Ab-3 and Ab-5 monoclonal antibodies. (**B**) Overnight serum-starved SK-Br3 breast cancer cells were cultured in IMEM-0.1% FBS supplemented with 20 μM orlistat for 48 h. The amount of cell surface-associated $p185^{Her2/neu}$ was quantified by flow cytometric analyses using a specific antibody against the extracellular domain of Her2/*neu* (Ab-5) as described in Materials and methods. The mean fluorescence signal ± SD ($n = 3$) was quantified using the geo mean (GM) fluorescence parameter provided with the Cell Quest Software (Becton Dickinson). (**C**) Impact of orlistat-induced inhibition of FAS activity on $p185^{Her2/neu}$ cellular localization. Untreated (panel i) and orlistat-treated (panel ii) SK-Br3 cells were fixed, permeabilized, and labeled with the $p185^{Her2/neu}$ Ab-3 monoclonal antibody. Cellular localization of $p185^{Her2/neu}$ was detected by indirect immunofluorescence by incubating with TRITC-conjugated anti-mouse IgG. After counterstaining with DAPI, cells were examined and photographed by using a Zeiss fluorescent microscope. A representative immunostaining analysis ($n = 3$) is shown. (**D**) Overnight-serum starved SK-Br3 cells were cultured in IMEM-0.1% FBS supplemented with increasing concentrations of orlistat for 48 h, and the harvested and lysed as described in Materials and methods. Equal amounts of protein were subjected to western blot analyses with a specific antibody against either $p185^{Her2/neu}$ (Ab-3) or PEA3, and then re-probed with a β-actin antibody. The figure shows a representative immunoblotting analysis ($n = 3$). (**E**) Orlistat represses Her2/*neu* promoter activity through a positive regulatory PEA3-binding DNA motif. Luciferase reporter gene driven by either wild-type (left panel) or the PEA3 site-mutated (right panel) Her2/*neu* promoter was measured after treatment with either 10 μM

orlistat-induced inhibition of FAS activity in the subcellular localization of $p185^{Her2/neu}$. To address this question, orlistat-treated SK-Br3 cells were permeabilized with Triton X-100 for the intracellular delivery of antibodies directed against the extracellular domain and the carboxy terminal 14 cytoplasmic amino acids of $p185^{Her2/neu}$ (Ab-5 and Ab-3, respectively; Figure 3A). Untreated cells showed a prominent cell-surface staining of $p185^{Her2/neu}$ (Figure 3C, panel i). Upon orlistat treatment, the membrane staining of $p185^{Her2/neu}$ was clearly diminished when the subcellular localization of $p185^{Her2/neu}$ was assessed with wither Ab-5 (data not shown) or Ab-3 (Figure 3C, panel ii). Although $p185^{Her2/neu}$ was somewhat distributed through the cytoplasm in orlistat-treated SK-Br3 cells, we failed to observe a prominent nuclear accumulation of $p185^{Her2/neu}$ as we previously reported in Her2/*neu*-overexpressing cancer cells treated with the FAS blocker C75 [33]. A significant decrease in the expression of Her2/*neu*-coded $p185^{Her2/neu}$ oncoprotein was also observed in Western blotting analyses of cell lysates from orlistat-treated SK-Br3 cells using the Ab-3 monoclonal antibody recognizing the carboxyl terminal 14 amino acids of $p185^{Her2/neu}$ (Figure 3D). Equivalent results were found in Her2/*neu*-overexpressing BT-474 breast cancer cells (data not shown). These findings support the notion that Her2/*neu* oncogene may act as the key molecular sensor of energy imbalance after the perturbation of FAS activity in cancer cells [33].

Orlistat inhibits Her2/*neu* promoter activity through the *Ets* transcription factor PEA3

To characterize the specific mechanism through which orlistat-induced inhibition of FAS activity molecularly modulated Her2/*neu* oncogene expression, we performed transient transfection experiments with a luciferase reporter gene driven by the Her2/*neu* promoter (pNulit). Remarkably, orlistat treatment was found to profoundly repress the activity of Her2/*neu* gene promoter (up to 60% inhibition) in SK-Br3 breast cancer cells (Figure 3E, left panel). We sought an independent means of inhibiting FAS to solidify the role of this enzyme in regulating Her2/*neu* promoter activity. Therefore, we compared orlistat and siRNA-targeting FAS for the ability to knock down the transcriptional activation of Her2/*neu* gene in SK-Br3 breast cancer cells. RNAi-mediated silencing of FAS reduced the level of FAS protein [33] and likewise down-regulated Her2/*neu* promoter activity by about 50% (Figure 3E, left panel). Together, these findings provide strong support for the idea that a FAS blockade in breast cancer cells acts upon Her2/*neu* oncogene expression, at least in part, via regulation of Her2/*neu* promoter activity.

To gain additional insight into the molecular mechanisms underlying the repression of Her2/*neu* promoter activity induced by orlistat, we examined the expression of Her2/*neu* regulator PEA3 following orlistat-induced blockade of FAS activity in SK-Br3 cells. The DNA-binding protein PEA3, a member of the *Ets* transcription factor family, specifically targets a DNA sequence on the Her2/*neu* promoter and down-regulates its promoter activity thus suppressing Her2/*neu* overexpression and inhibiting tumorigenesis [52, 58]. Interestingly, a significant accumulation of the DNA-binding protein PEA3 was observed following orlistat exposure (Figure 3D). Moreover, when orlistat's effects on the transcriptional activation of Her2/*neu* gene were characterized on a Her2/*neu* promoter bearing a mutated PEA3 binding sequence (5′-AGGAAG-3′ to 5′-AGCTCG-3′), the luciferase reporter gene driven by the PEA3 site-mutated sequence was not subject to negative regulation by either orlistat or siRNA FAS (Figure 3E, right panel). As previously demonstrated by Xing *et al.* in SKOV-3 and MDA-MB-453 cells [57], when the levels of wild-type and mutant Her2/*neu* promoter activities were compared in untreated control cells, the mutant promoter was significantly less active than the wild-type in SK-Br3 cells. These results, altogether, strongly suggest that orlistat, through its FAS target, represses Her2/*neu* promoter activity through a positive regulatory PEA3-binding DNA motif. Equivalent results were found in Her2/*neu*-overexpressing BT-474 breast cancer cells (data not shown).

Orlistat co-exposure synergistically enhances trastuzumab efficacy in Her2/*neu*-overexpressing breast cancer cells

We explored whether the down-regulatory effects of orlistat on Her2/*neu* gene expression could modulate the growth inhibitory effects of trastuzumab (Herceptin™), a humanized monoclonal antibody binding with high affinity to the ectodomain of $p185^{Her2/neu}$ oncoprotein and showing encouraging therapeutic effects in patients with Her2/*neu*-overexpressing metastatic breast cancer [59–62]. Although there remains controversy over which method is best for detecting true *in vitro* synergy between drug combinations, the combined cytotoxic effect of orlistat and trastuzumab was assessed using the median-effect plot analysis of Chou and Talalay [35–37]. This procedure allows the characterization of drug interactions with a single number, the Combination Index (CI). The CI parameter indicates whether the doses of the two agents required to produce a given degree of cytotoxicity are greater than (CI >1 or antagonism) equal to (CI = 1 or addition) or less than (CI <1 or synergism) the doses that would be required if the two agents were strictly additive. For this type of analysis and for each drug separately (i.e. orlistat and trastuzumab), we measured how the fraction affected (i.e. the fractional cell toxicity) varied with differing doses. For two drugs in combination (i.e. orlistat + trastuzumab, orlistat → trastuzumab or trastuzumab → orlistat) we varied the doses

orlistat or 200 nM siRNA-targeting FAS for 48 h. The activity of the wild-type promoter in the absence of treatments was defined as 100%. Values shown are means (columns) ± SD (bars) from triplicate wells, and are representative of repeated experiments. Student's *t*-test was used to evaluate the statistical significance of mean values. Statistical significance level was $P < 0.005$ (denoted as **).

of the two agents while monitoring the fraction affected; however, the doses were varied such that a constant ratio of agent 1 (orlistat) to agent 2 (trastuzumab) was maintained. Specifically, 1.5, 2.0- and 3.0-fold serial dilutions of orlistat and trastuzumab were prepared and combined with each other from the lowest to the highest concentration while assessing the cell fraction affected. The combination ratio was designed to approximate the IC_{50} ratio of the drugs determined in preliminary experiments, so that the contribution of the effect for orlistat and trastuzumab in the mixture would be the same (i.e. equipotency ratio). Figure 4A shows the CI plots at various effect levels (fraction affected) for the combination of orlistat and trastuzumab in SK-Br3 cells using different schedules of administration. The synergy observed with concurrent orlistat and trastuzumab exposure for 96 h was apparent at all the levels of cell kill (10%, 30%, 50%, 70% and 90%), with CI values ranging from 0.110 (strong synergism) to 0.847 (moderate synergism). Although the CI values obtained in SK-Br3 cells exposed for 48 h to orlistat before exposure to trastuzumab for 48 h also suggested a synergistic effect under this sequential schedule (CI = 0.380 at the IC_{10}, CI = 0.514 at the IC_{30}), this regimen became additive and slightly antagonist at levels exceeding the 50% cell kill boundary (CI = 1.210 at the IC_{90}). These findings suggest that co-exposure of Her2/*neu*-overexpressing SK-Br3 cells to FAS inhibitor orlistat and anti-Her2/*neu* antibody trastruzumab is necessary for maximal augmentation of cytotoxicity, whereas sequential administration of trastuzumab followed by orlistat significantly reduces the synergism between the two agents.

To determine whether the synergy between orlistat and trastuzumab was accompanied with an increase in the extent of apoptosis, SK-Br3 cells were exposed to trastuzumab in the absence or presence of increasing concentrations of orlistat, cell death was measured by an ELISA that detected DNA-histone fragmentation, and the *x*-fold increase in apoptotis-related cell death was calculated by comparing the ELISA optical density reading of treated samples with the values of untreated cells as 1.0. SK-Br3 cells co-treated with trastuzumab and orlistat exhibited a higher degree of cell death compared with that observed when trastuzumab and orlistat were used as single agents (Figure 4B). Therefore, the increased sensitivity to trastuzumab seen in orlistat-treated SK-Br3 cells is not simply the result of changes in cell proliferation, but might actually be due to increases in apoptotic cell death following orlistat-induced cell damage.

High levels of FAS determine breast cancer cell hypersensitivity to orlistat

We finally characterized the relationship between the cytotoxic effects of orlistat and the expression of FAS in a panel of human breast cancer cell lines. Cells were seeded in microtiter plates and then cultured in the absence or presence of increasing concentrations of orlistat until untreated cells reached confluence. Then, the metabolic status of breast cancer cells was judged by the mitochondrial conversion of the tetrazolium salt, MTT, to its formazan product (MTT assay). Concentration–effect curves were generated by

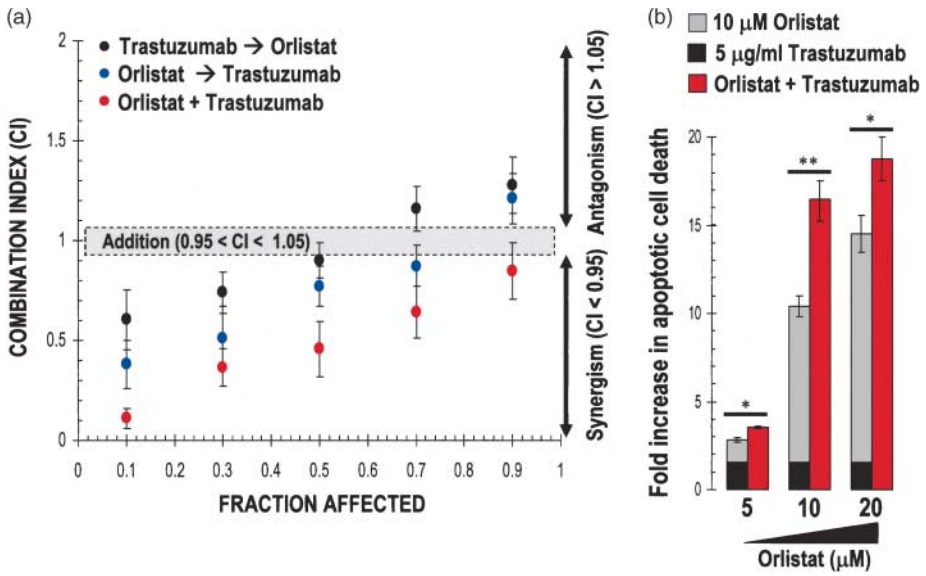

Figure 4. (**A**) Synergy analysis of the interaction between orlistat and trastuzumab against SK-Br3 cells according to the median-effect plot analysis of Chou and Talalay. Shown in the figure are plots of the combination index (CI) at various effect levels (fraction affected) for the combination of orlistat and trastuzumab in SK-Br3 cells using different schedules of administration. The CIs were calculated using assumptions for the drug both mutually exclusive. The shaded area indicates the addition area based on a null interval of 0.95–1.05. CIs above and below indicate antagonism and synergism, respectively. Results are means (dots) ± SD (bars) of three independent experiments made in triplicate. (**B**) Concurrent exposure to orlistat and trastuzumab (Herceptin™) synergistically induces apoptotic breast cancer cell death. The induction of apoptosis by exposure of SK-Br3 cells for 72 h with the indicated doses of orlistat, trastuzumab, and/or orlistat *plus* trastuzumab was assessed using the Cell Death Detection ELISA^{PLUS} kit obtained from Roche Molecular Biochemicals USA (Indianapolis, IN, USA) exactly as described in the manufacturer's protocol. The Student's *t*-test was used to evaluate the statistical significance of mean values. Statistical significance levels were $P < 0.05$ (denoted as ∗) and $P < 0.005$ (denoted as ∗∗).

plotting the fraction of unaffected (surviving) cells versus orlistat concentration, and IC_{50} values (the doses of orlistat producing a 50% reduction in cell viability) were calculated as described in Material and methods. Breast cancer cell lines exhibiting IC_{50} values >20 μM for orlistat were arbitrarily defined as 'low-sensitive', whereas those exhibiting IC_{50} values <5 μM were defined as 'high-sensitive' (Figure 5A, bottom panel). When the status of FAS expression (as assessed by western blotting using a monoclonal antibody against FAS (Figure 5A, top panel) was correlated to the sensitivity profile of breast cancer cells to orlistat-induced cytotoxicity, we found that Her2/*neu*- and FAS-overexpressing SK-Br3 and BT-474 cells were significantly more sensitive to orlistat than others, with IC_{50}s of 7.5 ± 3 and 10 ± 1 μM, respectively. Moderately FAS-expressing MDA-MB-453 and T47D cells, which exhibit high and moderate levels of Her2/*neu*, respectively, demonstrated an intermediate profile of sensitivity to orlistat, with IC_{50}s of 13 ± 2 and 12 ± 2 μM. Her2/*neu*-negative and low-FAS-expressing MDA-MB-435 and MDA-MB-231 exhibited the highest IC_{50} values for orlistat (23 ± 3 and 21.5 ± 4 μM, respectively). This analysis clearly established that the cytotoxic effects of orlistat correlate, indeed, with constitutive FAS expression levels in breast cancer cells.

To conclusively confirm the selectivity of orlistat toward FAS and Her2/*neu* overexpressors, we analyzed the cytotoxic effects of orlistat following the forced expression of Her2/*neu* oncogene in MCF-7 breast cancer cells, which naturally express moderate levels of both FAS and Her2/*neu* [29]. In this scenario, we recently demonstrated that transfection with the full-length cDNA of the human Her2/*neu* oncogene results in a significant enhancement of activation of a FAS promoter–reporter construct up to three-fold higher than that found in wild-type MCF-7 cells [32] which, in turn, induces a significant accumulation of FAS protein compared with matched control MCF-7/neo cells (Figure 5B, top panel). Interestingly, MCF-7/Her2-18 cells were noticeably more sensitive to orlistat-induced cytotoxicity compared with control cells, and the magnitude of this sensitization (up to 2.5-fold) did correlate with the level of Her2/*neu*-promoted up-regulation of FAS expression (Figure 5B, bottom panel). These studies support the argument that Her2/*neu* overexpression, through its ability to stimulate FAS expression may be sufficient to induce a greater sensitivity of breast cancer cells to orlistat.

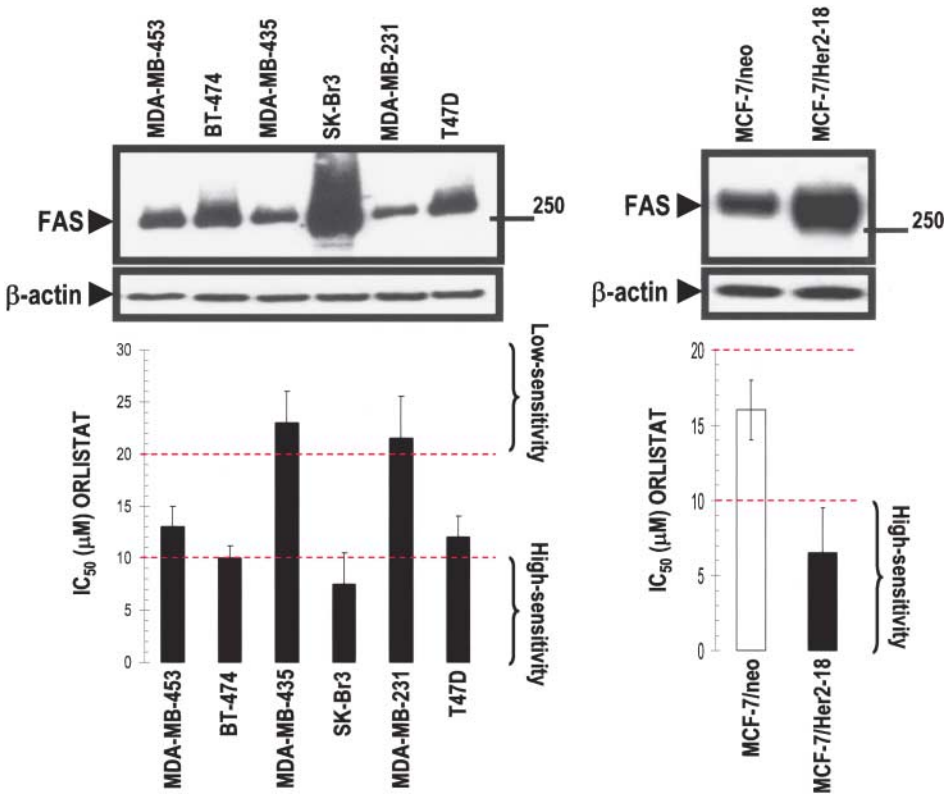

Figure 5. Breast cancer cell sensitivity to orlistat positively correlates with FAS (orlistat's target) protein expression. Top panels: FAS protein expression in a panel of human breast cancer cell lines. MDA-MB-453, BT-474, MDA-MB-435, SK-Br3, MDA-MB-231, T47D, MCF-7/neo and MCF-7/Her2-18 cells were grown in IMEM-5% FBS until reaching 75% confluence. Cells were then washed with PBS and solubilized in lysis buffer as described in Materials and methods. Aliquots (10 μg) of 14 000 × *g* supernatants were fractioned by NuPAGE, transferred to nitrocellulose membranes, probed with an anti-FAS monoclonal antibody, and then re-probed with a β-actin antibody. Figure shows a representative immunoblotting analysis ($n = 3$). Bottom panels: for each cell line, cell viability curves following exposure to orlistat were constructed as described in Materials and methods. Breast cancer cell sensitivity to orlistat was expressed in terms of the concentration of orlistat required for 50% (IC_{50}) reduction of cell viability. Values shown are means (columns) ± SD (bars) of repeated experiments ($n = 4$).

Discussion

The lipogenic enzyme FAS, also called oncogenic antigen-519, is selectively and highly expressed in virulent breast cancers [8, 9, 63, 64]. In two separated studies that examined stage I (<2 cm, negative axillary lymph nodes) breast carcinoma patients, high FAS expression was associated with a four-fold increase in risk of death [8, 9]. Remarkably, the differential expression of FAS between cancer and normal cells may provide a useful drug target for the development of novel therapeutic anti-metabolites [41]. Previous studies of intratumoral injection of the natural FAS blocker cerulenin demonstrated local efficacy of FAS inhibition against a human cancer xenograft but were limited to the failure of cerulenin to act systemically [65]. Recently, Kuhajda and co-workers described the *de novo* synthesis of a synthetic, chemically stable inhibitor of mammalian FAS, C75, based on the known mechanism of action of cerulenin [40]. C75 treatment of MCF-7 human breast cancer xenografts showed significant antitumor activity with concomitant inhibition of fatty acid synthesis in tumor tissue and normal liver [66]. Importantly, histopathological analysis of normal tissues after C75 treatment showed no adverse effects on proliferating cellular compartments, such as bone marrow, gastrointestinal tract, skin or lymphoid tissues. Moreover, the primary mechanism of the antitumor activity of C75 was mediated through its interaction, and inhibition of, FAS. Thus, increasing bodies of *in vitro* and *in vivo* evidence strongly suggest that pharmacological inhibition of FAS represents a novel therapeutic approach in human breast cancer. Unfortunately, cerulenin and C75 are now known to have other molecular targets [67–69], so searches for additional antagonists of FAS with better selectivity and distinct mechanisms of action are warranted.

Our study confirms that micromolar concentrations of orlistat, a drug approved for treating obesity and recently characterized as a potent and selective inhibitor of FAS in prostate carcinoma cells [3], induce potent anti-proliferative and apoptotic effects in breast cancer cells through its ability to block the lipogenic activity of FAS. These results not only reinforce the notion that breast cancer-associated FAS activity is a relevant molecular target for drug development in oncology, but further demonstrate a close involvement of Her2/*neu* (*erb* B-2) oncogene, the overexpression and/or activation of which is known to play an important role in the etiology, aggressive progression and poor clinical outcome of breast carcinomas. Thus, when we characterized signaling molecules participating in the cellular events that followed orlistat-induced inhibition of FAS activity and preceded inhibition of breast cancer cell proliferation, orlistat treatment was found to dramatically suppress Her2/*neu* expression in SK-Br3 and BT-474 cell lines, two *in vitro* models of FAS and Her2/*neu*-overexpressing breast cancer [29]. This observation supports our prior work in which pharmacological and RNAi-mediated blockade of FAS signaling was found to suppress Her2/*neu* overexpression in cancer cells [33]. Indeed, the ability of orlistat to deplete Her2/*neu* oncoprotein in breast cancer cells constitutes an independent strategy to confirm that FAS inhibition, regardless of the mechanism of action of the chemical FAS blocker, is accompanied by the specific suppression of Her2/*neu* oncogene. These findings strongly support the idea that breast cancer-associated FAS is not a mere manifestation of early and common cancer-associated epigenetic changes but rather actively contributes to the breast cancer phenotype by regulating the expression, activity and cellular localization of Her2/*neu* oncogene [16, 33, 34].

The present study also provides new insight into the mechanisms underlying the connection between breast cancer-associated FAS and Her2/*neu* oncogene. Unlike the humanized anti-Her2/*neu* monoclonal antibody trastuzumab (Herceptin™), which targets the ectodomain of Her2/*neu* receptor and promote its degradation, FAS blockade appears to mitigate Her2/*neu* overexpression, at least in part, *via* PEA3 binding to the Her2/*neu* promoter, thus suppressing its transcriptional activity. Therefore, this distinct mechanism of action should not be affected by the mechanisms of resistance described for trastuzumab-based anti-Her2/*neu* immunotherapy [70–73]. Moreover, orlistat-induced inhibition of FAS activity significantly enhanced the anti-proliferative effects of trastuzumab. To evaluate the nature of the interaction following three different schedules of administration (orlistat + trastuzumab, orlistat → trastuzumab and trastuzumab → orlistat), which might be synergistic, additive or antagonistic, we used the Chou and Talalay analysis, a mathematical method employed for assessing the combined effect of antitumor drugs *in vitro* as a preclinical screening test [35–37]. Our studies demonstrated that the greatest number of synergistic combinations as well as the greatest magnitude of synergy was observed when Her2/*neu*- and FAS-overexpressing SK-Br3 breast cancer cells were exposed to the two agents simultaneously, whereas additive or even antagonistic interactions were observed when either FAS blocker orlistat preceded trastuzumab or trastuzumab preceded orlistat, respectively. Indeed, orlistat-induced transcriptional repression of Her2/*neu* gene, when concurrently combined with sub-optimal concentrations of trastuzumab, was able to promote high levels of apoptotic cell death in Her2/*neu*-overexpressing breast cancer models. From a clinical perspective, these findings suggest that the simultaneous administration of orlistat-related anti-FAS compounds and trastuzumab may be the optimal schedule for the combination in terms of cytotoxic effects. Although the ultimate molecular mechanisms of interaction operating with these schedules were not conclusively addressed by our experiments, these events may be related to the relative output of Her2/*neu*-driven signaling in breast cancer cells. We recently demonstrated that the synergistic inhibition of breast cancer cell viability following the concomitant targeting of Her2/*neu* and FAS using sub-optimal doses of trastuzumab and chemical FAS blockers cerulenin and C75 was accompanied by a dramatic reduction on Her2/*neu* expression levels [33]. This strongly suggests a novel role of Her2/*neu* as a key molecular sensor of the energy imbalance that follows perturbation of cancer-associated endogenous fatty acid metabolism. Our current approach further demonstrates

that the simultaneous combination of a FAS inhibitor, such as orlistat and trastuzumab, is more effective than the single treatments in inducing cytotoxicity and apoptotic cell death toward Her2/*neu*-overexpressing breast cancer cells. These findings support the clinical potential of concurrent treatments using FAS blockers, which seem to repress Her2/*neu* oncogene expression at the transcriptional levels by up-regulating PEA3, and monoclonal antibodies to Her2/*neu* such as trastuzumab, which targets the ectodomain of $p185^{Her2/neu}$ and promotes Her2/*neu* protein degradation [74–76]. Pre-exposure to orlistat does not affect FAS expression [3], while significantly down-regulating Her2/*neu* expression. This, in turn, may raise the sensitivity threshold for trastuzumab-induced cell growth inhibition, then contributing to the observed reduction of synergism under a sequential schedule orlistat → trastuzumab. Pre-exposure to trastuzumab not only reduces $p185^{Her2/neu}$ but further down-regulates FAS [30, 31]. Under these conditions, trastuzumab pretreatment not only decreases the levels of orlistat's target (i.e. FAS) but further blocks one of the molecular mechanisms through which FAS blockade promotes breast cancer cell toxicity (i.e. Her2/*neu* down-regulation). Accordingly, the trastuzumab → orlistat schedule yields the highest CI (i.e. antagonistic) values in all the combinations tested for orlistat and trastuzumab. Nonetheless, considering that preclinical studies clearly indicate that transcriptional repressors that down-regulate Her2/*neu* promoter activity can be effective regimens for cancer treatment [77], if chemically stable FAS inhibitors or cancer cell-selective vector systems able to deliver RNAi targeting FAS gene demonstrates systemic anticancer effects *in vivo*, our results render FAS as a promising therapeutic target to influence the outcome of Her2/*neu*-overexpressing breast carcinomas.

Recent experimental and epidemiological data strongly suggested a protective effect of statins on cancer and further support a role of statins in chemoprevention and, perhaps, treatment of cancer disease [78–81]. The molecular mechanisms underlying the anticancer activity of different statins, however, remain largely uncertain. The ability of statins such as simvastatin to block the enzymatic activity of 3-hydroxy-3-methylglutaryl-coenzyme A reductase, might prevent the expression of the oncogenic phenotype by blocking the activation of oncoproteins such as *k*-Ras [78–81]. This mechanism of action, however, should not affect the transcription of oncogenes and, therefore, precludes the potential of simvastatin-related statins to affect the malignant phenotype. However, orlistat actively regulates the malignant phenotype of breast cancer cells as it suppresses Her2/*neu* oncogene expression by blocking the lipogenic activity of FAS. Though orlistat possess extremely low oral bioavailability, it is obvious that a novel formulation and/or route of administration will be required for treating tumors such breast carcinomas. In its approved formulation orlistat is administered orally, which could be useful in treating tumors of the gastrointestinal (GI) tract. Interestingly, we have recently found orlistat to block Her2/*neu* overexpression and induce apoptosis in the highly-metastatic NCI-N87 stomach carcinoma cell line [82], thus suggesting that this selective lipase inhibitor used for treating obesity may represent a suitable drug candidate for treating Her2/*neu*-overexpressing GI carcinomas through its ability to block cancer-associated FAS hyperactivity. Moreover, future analyses of the incidence and clinical outcome of gastrointestinal carcinomas in a representative obese population earlier receiving orlistat treatment, may illustrate further its chemopreventive effects to GI cancers. Nevertheless, its potent pro-apoptotic activity, which is accompanied by a dramatic down-regulation of Her2/*neu* oncogene, and the synergistic interaction that occurs following co-treatment with orlistat and trastuzumab, cannot exclude the notion that more potent or bioavailable variants of orlistat and/or orlistat-related β-lactones as suitable drug candidates for treating Her2/*neu*-overexpressing breast carcinomas.

Acknowledgements

The authors wish to thank Mien-Chie Hung (The University of Texas M.D. Anderson Cancer Center, Department of Cancer Biology, Section of Molecular Cell Biology, Houston, Texas, USA) for kindly providing Her2/*neu* promoter constructs. Javier A. Menendez is the recipient of a Translational Research Pilot Project (PP2) and of a Career Development Award from the Specialized Program of Research Excellence (SPORE) in Breast Cancer (Robert H. Lurie Comprehensive Cancer Center, Chicago, USA), of a Basic, Clinical and Translational Award (BRCTR0403141) from the Susan G. Komen Breast Cancer Foundation (USA), and of a Breast Cancer Concept Award (BC033538) from the Department of Defense (DOD, USA).

References

1. McNeely W, Benfield P. Orlistat. Drugs 1998; 56: 241–249.
2. Hadvary P, Sidler W, Meister W et al. The lipase inhibitor tetrahydrolipstatin binds covalently to the putative active site serine of pancreatic lipase. J Biol Chem 1991; 266: 2021–2027.
3. Kridel SJ, Axelrod F, Rozenkrantz N, Smith JW. Orlistat is a novel inhibitor of fatty acid synthase with antitumor activity. Cancer Res 2004; 64: 2070–2075.
4. Tsukamoto Y, Wong H, Mattick JS, Wakil SJ. The architecture of the animal fatty acid synthetase complex. IV. Mapping of active centers and model for the mechanism of action. J Biol Chem 1983; 258: 15312–15322.
5. Joshi AK, Witkowski A, Smith S. Mapping of functional interactions between domains of the animal fatty acid synthase by mutant complementation *in vitro*. Biochemistry 1997; 36: 2316–2322.
6. Chirala SS, Jayakumar A, Gu ZW, Wakil S. Human fatty acid synthase: role of interdomain in the formation of catalytically active synthase dimmer. Proc Natl Acad Sci USA 2001; 98: 3104–3108.
7. Rangan VS, Joshi AK, Smith S. Mapping the functional topology of the animal fatty acid synthase by mutant complementation in vitro. Biochemistry 2001; 40: 10792–10799.
8. Alo PL, Visca P, Marci A et al. Expression of fatty acid synthase (FAS) as a predictor of recurrence in stage I breast carcinoma patients. Cancer 1996; 77: 474–482.

9. Alo PL, Visca P, Trombetta G et al. Fatty acid synthase (FAS) predictive strength in poorly differentiated early breast carcinomas. Tumori 1999; 85: 35–40.
10. Wang Y, Kuhajda FP, Li JN et al. Fatty acid synthase (FAS) expression in human breast cancer cell culture supernatants and in breast cancer patients. Cancer Lett 2001; 167: 99–104.
11. Wang YY, Kuhajda FP, Li J et al. Fatty acid synthase as a tumor marker: its extracellular expression in human breast cancer. J Exp Ther Oncol 2004; 4: 101–110.
12. Nakamura I, Kimijima I, Zhang GJ et al. Fatty acid synthase expression in Japanese breast carcinoma patients. Int J Mol Med 1999; 4: 381–387.
13. Milgraum LZ, Witters LA, Pasternack GR, Kuhajda FP. Enzymes of the fatty acid synthesis pathway are highly expressed in in situ breast carcinoma. Clin Cancer Res 1997; 3: 2115–2120.
14. Alo PL, Visca P, Botti C et al. Immunohistochemical expression of human erythrocyte glucose transporter and fatty acid synthase in infiltrating breast carcinomas and adjacent typical/atypical hyperplastic or normal breast tissue. Am J Clin Pathol 2001; 116: 129–134.
15. Kuhajda FP. Fatty-acid synthase and human cancer: new perspectives on its role in tumor biology. Nutrition 2000; 16: 202–208.
16. Menendez JA, Lupu R. Fatty acid synthase-catalyzed de novo fatty acid biosynthesis: from anabolic-energy-storage pathway in normal tissues to jack-of-all-trades in cancer cells. Arch Immunol Ther Exp (Warsz) 2004; 52: 414–426.
17. Menendez JA, Colomer R, Lupu R. Obesity, fatty acid synthase, and cancer: serendipity or forgotten causal linkage? Mol Genet Metab 2004; (In press; available online 9 December 2004).
18. Calle EE, Rodriguez C, Walker-Thurmond K, Thun MJ. Overweight, obesity, and mortality from cancer in a prospectively studied cohort of U.S. adults. N Engl J Med 2003; 348: 1625–1638.
19. Calle EE, Kaaks R. Overweight, obesity and cancer: epidemiological evidence and proposed mechanisms. Nat Rev Cancer 2004; 4: 579–591.
20. Loftus TM, Jaworsky DE, Frehywot GL et al. Reduced food intake and body weight in mice treated with fatty acid synthase inhibitors. Science 2000; 288: 2379–2381.
21. Bouchard C. Inhibition of food intake by inhibitors of fatty acid synthase. N Engl J Med 2000; 343: 1888–1889.
22. Mobbs CV, Makimura H. Block the FAS, lose the fat. Nat Med 2002; 8: 335–336.
23. Wang X, Tian W. Green tea epigallocatechin gallate: a natural inhibitor of fatty-acid synthase. Biochem Biophys Res Commun 2001; 288: 1200–1206.
24. Brusselmans K, De Schrijver E, Heyns W et al. Epigallocatechin-3-gallate is a potent natural inhibitor of fatty acid synthase in intact cells and selectively induces apoptosis in prostate cancer cells. Int J Cancer 2003; 106: 856–862.
25. Yeh CW, Chen WJ, Chiang CT et al. Suppression of fatty acid synthase in MCF-7 breast cancer cells by tea and tea polyphenols: a possible mechanism for their hypolipidemic effects. Pharmacogenomics J 2003; 3: 267–276.
26. Slamon DJ. Proto-oncogenes and human cancers. N Engl J Med 1987; 317: 955–957.
27. Slamon DJ, Godolphin W, Jones LA et al. Studies of the HER2/*neu* proto-oncogene in human breast and ovarian cancer. Science 1989; 244: 707–712.
28. Marmor MD, Skaria KB, Yarden Y. Signal transduction and oncogenesis by ErbB/HER receptors. Int J Radiat Oncol Biol Phys 2004; 58: 903–913.
29. Menendez JA, Mehmi I, Atlas E et al. Novel signaling molecules implicated in tumor-associated fatty acid synthase-dependent breast cancer cell proliferation and survival: role of exogenous dietary fatty acids, p53-p21WAF1/CIP1, ERK1/2 MAPK, p27KIP1, BRCA1, and NF-kappaB. Int J Oncol 2004; 24: 591–608.
30. Kumar-Sinha C, Ignatoski KW, Lippman ME et al. Transcriptome analysis of HER2 reveals a molecular connection to fatty acid synthesis. Cancer Res 2003; 63: 132–139.
31. Menendez JA, Ropero S, Mehmi I et al. Overexpression and hyperactivity of breast cancer-associated fatty acid synthase (oncogenic antigen-519) is insensitive to normal arachidonic fatty acid-induced suppression in lipogenic tissues but it is selectively inhibited by tumoricidal alpha-linolenic and gamma-linolenic fatty acids: a novel mechanism by which dietary fat can alter mammary tumorigenesis. Int J Oncol 2004; 24: 1369–1383.
32. Menendez JA, Decker JP, Lupu R. In support of fatty acid synthase (FAS) as a metabolic oncogene: extracellular acidosis acts in an epigenetic fashion activating FAS gene expression in cancer cells. J Cell Biochem 2005; 94: 1–4.
33. Menendez JA, Vellon L, Mehmi I et al. Inhibition of fatty acid synthase (FAS) suppresses HER2/neu (erbB-2) oncogene overexpression in cancer cells. Proc Natl Acad Sci USA 2004; 101: 10715–10720.
34. Menendez JA, Mehmi I, Verma VA et al. Pharmacological inhibition of fatty acid synthase (FAS): a novel therapeutic approach for breast cancer chemoprevention through its ability to suppress Her2/neu (erbB-2) oncogene-induced malignant transformation. Mol Carcinog 2004; 41: 164–178.
35. Chou TC, Talalay P. Quantitative analysis of dose-effect relationships: the combined effects of multiple drugs or enzyme inhibitors. Adv Enzyme Regul 1984; 22: 27–55.
36. Chou J, Chou TC. Quantitation of synergism and antagonism of two or more drugs by computerized analysis. In Chou TC, Rideout DC (eds): Synergism and Antagonism in Chemotherapy. San Diego, CA: Academic Press 1991; 223–244.
37. Chou TC, Motzer RJ, Tong Y, Bosl GJ. Computerized quantitation of synergism and antagonism of Taxol™, topotecan and cisplatin against teratocarcinoma cell growth: a rational approach to clinical protocol design. J Natl Cancer Inst 1994; 86: 1517–1524.
38. Mattick JS, Nickless J, Mizugaki M et al. The architecture of the animal fatty acid synthetase. II. Separation of the core and thioesterase functions and determination of the N-C orientation of the subunit. J Biol Chem 1983; 258: 15300–15304.
39. Moche M, Schneider G, Edwards P et al. Structure of the complex between the antibiotic cerulenin and its target, b-ketoacyl-acyl carrier protein synthase. J Biol Chem 1999; 274: 6031–6034.
40. Kuhajda FP, Pizer ES, Li JN et al. Synthesis and antitumor activity of an inhibitor of fatty acid synthase. Proc Natl Acad Sci USA 2000; 97: 3450–3454.
41. Kuhajda FP, Jenner K, Wood FD et al. Fatty acid synthesis: a potential selective target for antineoplastic therapy. Proc Natl Acad Sci USA 1994; 91: 6379–6383.
42. Pizer ES, Jackisch C, Wood FD et al. Inhibition of fatty acid synthesis induces programmed cell death in human breast cancer cells. Cancer Res 1996; 56: 2745–2747.
43. Pizer ES, Chrest FJ, DiGiuseppe JA, Han WF. Pharmacological inhibitors of mammalian fatty acid synthase suppress DNA replication and induce apoptosis in tumor cell lines. Cancer Res 1998; 58: 4611–4615.
44. Li JN, Gorospe M, Chrest FJ et al. Pharmacological inhibition of fatty acid synthase activity produces both cytostatic and cytotoxic effects modulated by p53. Cancer Res 2001; 61: 1493–1499.
45. Alli PM, Pinn ML, Jaffee EM et al. Fatty acid synthase inhibitors are chemopreventive for mammary cancer in neu-N transgenic mice. Oncogene 2004; [Epub ahead of print].

46. Knowles LM, Axelrod F, Browne CD, Smith JW. A fatty acid synthase blockade induces tumor cell-cycle arrest by down-regulating Skp2. J Biol Chem 2004; 279: 30540–30545.
47. Pizer ES, Wood FD, Pasternack GR, Kuhajda FP. Fatty acid synthase (FAS): a target for cytotoxic antimetabolites in HL60 promyelocytic leukemia cells. Cancer Res 1996; 56: 745–751.
48. Jackowski S, Wang J, Baburina I. Activity of the phosphatidylcholine biosynthetic pathway modulates the distribution of fatty acids into glycerolipids in proliferating cells. Biochim Biophys Acta 2000; 1483: 301–315.
49. Jackowski S. Coordination of membrane phospholipid synthesis with the cell cycle. J Biol Chem 1994; 269: 3858–3867.
50. Kaufmann SH, Desnoyers S, Ottaviano Y et al. Specific proteolytic cleavage of poly(ADP-ribose) polymerase: an early marker of chemotherapy-induced apoptosis. Cancer Res 1993; 53: 3976–3985.
51. Lazebnik YA, Kaufmann SH, Desnoyers S et al. Cleavage of poly(-ADP-ribose) polymerase by a proteinase with properties like ICE. Nature 1994; 371: 346–357.
52. Oliver FJ, de la Rubia G, Rolli V et al. Importance of poly(ADP-ribose) polymerase and its cleavage in apoptosis. Lesson from an uncleavable mutant. J Biol Chem 1998; 273: 33533–33539.
53. Shah GM, Kaufmann SH, Poirier GG. Detection of poly(ADP-ribose) polymerase and its apoptosis-specific fragment by a nonisotopic activity-western blot technique. Anal Biochem 1995; 232: 251–254.
54. Li X, Darzynkiewicz Z. Cleavage of poly(ADP-ribose) polymerase measured in situ in individual cells: relationship to DNA fragmentation and cell cycle position during apoptosis. Exp Cell Res 2000; 255: 125–132.
55. Xie Y, Hung MC. Nuclear localization of p185neu tyrosine kinase and its association with transcriptional transactivation. Biochem Biophys Res Commun 1994; 203: 1589–1598.
56. Wang SC, Lien HC, Xia W et al. Binding at and transactivation of the COX-2 promoter by nuclear tyrosine kinase receptor ErbB-2. Cancer Cell 2004; 6: 251–261.
57. Xing X, Wang SC, Xia W et al. The ets protein PEA3 suppresses HER2/neu overexpression and inhibits tumorigenesis. Nat Med 2000; 6: 189–195.
58. Wang SC, Hung MC. Transcriptional targeting of the HER2/neu oncogene. Drugs Today (Barc) 2000; 36: 835–843.
59. Vogel CL, Cobleigh MA, Tripathy D et al. First-line herceptin monotherapy in metastatic breast cancer. Oncology 2001; 61 (Suppl 2): 37–42.
60. Harries M, Smith I. The development and clinical use of trastuzumab (herceptin). Endocr Relat Cancer 2002; 9: 75–85.
61. Arteaga CL, Moulder SL, Yakes FM. HER (erbB) tyrosine kinase inhibitors in the treatment of breast cancer. Semin Oncol 2002; 29 (3 Suppl 11): 4–10.
62. Atalay G, Cardoso F, Awada A, Piccart MJ. Novel therapeutic strategies targeting the epidermal growth factor receptor (EGFR) family and its downstream effectors in breast cancer. Ann Oncol 2003; 14: 1346–1363.
63. Jensen V, Ladekarl M, Holm-Nielsen P et al. The prognostic value of oncogenic antigen 519 (OA-519) expression and proliferative activity detected by antibody MIB-1 in node-negative breast cancer. J Pathol 1995; 176: 343–352.
64. Kuhajda FP, Piantadosi S, Pasternack GR. Haptoglobin-related protein (Hpr) epitopes in breast cancer as a predictor of recurrence of the disease. N Engl J Med 1989; 321: 636–641.
65. Pizer ES, Wood FD, Heine HS et al. Inhibition of fatty acid synthase delays disease progression in a xenograft model of ovarian cancer. Cancer Res 1996; 56: 1189–1193.
66. Pizer ES, Thupari J, Han WF et al. Malonyl-coenzyme-A is a potential mediator of cytotoxicity induced by fatty-acid synthase inhibition in human breast cancer cells and xenografts. Cancer Res 2000; 60: 213–218.
67. Thupari JN, Landree LE, Ronnett GV, Kuhajda FP. C75 increases peripheral energy utilization and fatty acid oxidation in diet-induced obesity. Proc Natl Acad Sci USA 2002; 99: 9498–9502.
68. Lawrence DS, Zilfou JT, Smith CD. Structure-activity studies of cerulenin analogues as protein palmitoylation inhibitors. J Med Chem 1999; 42: 4932–4941.
69. De Vos ML, Lawrence DS, Smith CD. Cellular pharmacology of cerulenin analogs that inhibit protein palmitoylation. Biochem Pharmacol 2001; 62: 985–995.
70. Lu Y, Zi X, Zhao Y et al. Insulin-like growth factor-I receptor signaling and resistance to trastuzumab (Herceptin). J Natl Cancer Inst 2001; 93: 1852–1857.
71. Lu Y, Zi X, Pollak M. Molecular mechanisms underlying IGF-I-induced attenuation of the growth-inhibitory activity of trastuzumab (Herceptin) on SKBR3 breast cancer cells. Int J Cancer 2004; 108: 334–341.
72. Nahta R, Takahashi T, Ueno NT et al. P27(kip1) down-regulation is associated with trastuzumab resistance in breast cancer cells. Cancer Res 2004; 64: 3981–3986.
73. Nagata Y, Lan KH, Zhou X et al. PTEN activation contributes to tumor inhibition by trastuzumab, and loss of PTEN predicts trastuzumab resistance in patients. Cancer Cell 2004; 6: 117–127.
74. Baselga J, Albanell J. Mechanism of action of anti-HER2 monoclonal antibodies. Ann Oncol 2001; 12 (Suppl 1): S35–S41.
75. Albanell J, Codony J, Rovira A et al. Mechanism of action of anti-HER2 monoclonal antibodies: scientific update on trastuzumab and 2C4. Adv Exp Med Biol 2003; 532: 253–268.
76. Baselga J, Albanell J, Molina MA, Arribas J. Mechanism of action of trastuzumab and scientific update. Semin Oncol 2001; 28 (5 Suppl 16): 4–11.
77. Wang SC, Zhang L, Hortobagyi GN, Hung MC. Targeting HER2: recent developments and future directions for breast cancer patients. Semin Oncol 2001; 28(6 Suppl 18): 21–29.
78. Chan KKW, Oza AM, Siu LL. The statins as anticancer agents. Clin Cancer Res 2003; 9: 10–19.
79. Jakobisiak M, Golab J. Potential antitumor effects of statins (Review). Int J Oncol 2003; 23: 1055–1069.
80. Graaf MR, Beiderbeck AB, Egberts AC et al. The risk of cancer in users of statins. J Clin Oncol 2004; 22: 2388–2394.
81. A role for statins in chemoprevention? Lancet Oncol 2004; 5: 391.
82. Menendez JA, Vellon L, Lupu R. Orlistat: from antiobesity drug to anticancer agent in Her2/neu (*erb*B-2)-overexpressing gastrointestinal tumors? Exp Biol Med (Maywood) 2005; 230: 151–154.